Joint Source-Channel Rate Allocation in Parallel Channels

Lingling Pu, *Student Member, IEEE*, Michael W. Marcellin, *Fellow, IEEE*, Ivan Djordjevic, *Member, IEEE*, Bane Vasic, *Senior Member, IEEE*, and Ali Bilgin, *Member, IEEE*

***Abstract*—A fast rate-optimal rate allocation algorithm is proposed for parallel transmission of scalable images in multichannel systems. Scalable images are transmitted via fixed-length packets. The proposed algorithm selects a subchannel, as well as a channel code rate for each packet, based on the signal-to-noise ratios (SNRs) of the subchannels. The resulting scheme provides unequal error protection of source bits and significant gains are obtained over equal error protection schemes. An application of the proposed algorithm to JPEG2000 transmission shows the advantages of exploiting differences in SNRs between subchannels. Multiplexing of multiple sources is also considered, and additional gains are achieved by exploiting information diversity among the sources.**

***Index Terms*—Joint source/channel coding, JPEG2000, parallel channels, rate allocation.**

I. Introduction

PARALLEL channels are often used in multimedia transmission for more reliable communication or more efficient bandwidth usage. For example, in wireless channels, fading, shadowing, or other sources of interference can cause fluctuation of channel quality. Data transmitted through such a channel may have large distortion, or even be completely useless, especially for error-sensitive sources, such as compressed images. Another example is an underwater acoustic channel. In such a channel, there exist frequency-dependent signal attenuation and multipath due to reflections from the surface and the bottom of the sea. Intersymbol interference (ISI) results from the nonideal channel frequency response, and a complex equalizer may be needed to compensate for channel distortion. Using multiple parallel channels is one approach to combat such problems. It has attracted significant research interest, and yielded many modern communications techniques, such as multicarrier modulation (MCM) or discrete multitone (DMT) [1], [2]. Those techniques are well known for their advantages of bandwidth efficiency, excellent ISI performance, and immunity to multipath fading or time dispersion.

Manuscript received October 16, 2006; revised May 10, 2007. This work was supported in part by the National Science Foundation under Grant CCR-9979310 and Grant ANI-0325979. Portions of this work were presented at the IS&T/SPIE 19th Annual Symposium on Electronic Imaging, San Jose, CA, January, 2007. The associate editor coordinating the review of this manuscript and approving it for publication was Dr. Aria Nosratinia.

The authors are with the Department of Electrical and Computer Engineering, University of Arizona, Tucson, AZ 85721 USA (e-mail: lpu@email.arizona.edu; marcellin@ece.arizona.edu; ivan@ece.arizona.edu; vasic@ece.arizona.edu; bilgin@ece.arizona.edu).

Digital Object Identifier 10.1109/TIP.2007.901810

Joint source-channel coding is another way to improve performance of multimedia transmission systems. Modern error correction codes (ECC) are widely used along with MCM techniques to lower error rates in communication systems. Rate allocation plays an important role in designing a high performance end-to-end system. A rate allocation scheme decides how to distribute available resources such as bandwidths or bit budgets between sources and error protection. Pradhan and Ramchandran [3] propose a multiresolution modulation to achieve unequal error protection (UEP) for different resolution layers, but within each layer, equal error protection (EEP) is assigned across subchannels. Cherriman *et al.* [4] propose to choose a modulation mode to maximize throughput while keeping estimated BER lower than a target BER for orthogonal frequency division multiplexing (OFDM)-based interactive video telephony. In addition to the frequency diversity provided by MCM, other diversities, such as space and time diversity, are also studied and utilized in communication systems. For example, optimal rate allocation is proposed in an OFDM system using space-time block codes by Song and Liu [5]. Parallel subchannels are assumed to have the same SNR. Sun *et al.* [6], [7] propose a fast joint source-channel rate allocation for the transmission of scalable images over space-time coded OFDM systems for a given average SNR (BER). Chan *et al.* [8] propose to combine multiple description coding and frequency diversity, optimizing for a given SNR.

The above algorithms can be categorized as aiming to optimize system performance for a given *average* SNR (over subchannels). Varying subchannel SNR is considered in some cases, but not fully utilized for a joint design. Transmission of a layered source over spectrally shaped channels using MCM is proposed by Zheng and Liu [9]. The source layers are predetermined before allocation. Subchannels are ordered by SNR and the earlier layers select subchannels of higher SNR. The number of subchannels used by each layer is governed by the length of that layer. Zhao *et al.* [10], [11] propose optimal rate and power allocations in multichannel systems. Subchannels are assigned to layered images/videos sequentially first, then rates and power levels are allocated jointly between channels.

Rate-based optimization for the single channel case has been proposed by Stankovic *et al.* [12]. In this paper, we tackle the problem of designing a rate-based optimization scheme for multiple parallel channels, where the potential of varying SNR over all subchannels is fully exploited for robust transmission of scalable sources via fixed-length packets. For each source packet, the proposed algorithm selects a subchannel among all available subchannels, and chooses a channel code rate, such that the expected length of the correctly received source data is maximized. Additionally, our algorithm can incorporate constraints on the number of packets that can be carried by any given channel. Such constraints can not be handled by the single channel solution. Additionally, we investigate transmitting multiple sources. Source multiplexing is introduced and combined with rate allocation to provide a more fair distribution of quality among transmitted sources in addition to minimizing the average MSE over all sources.

We verify the proposed algorithm for different channel models. Two models are chosen for this purpose. The first one is a model of independent parallel Gaussian channels. This model is chosen because it can represent a nonwhite Gaussian noise channel or other spectrally shaped channels arising in various applications, such as DMT or MCM, multiple input multiple output (MIMO) systems, and OFDM, etc. OFDM is a special case of MCM. Coded OFDM (COFDM) has been specified for digital audio broadcasting (DAB) [13] and digital video television (DVB-T) [14]. The second model is chosen to demonstrate the suitability of the proposed scheme in a specific channel. To this end, a plastic optical fiber (POF) model is selected. POF is a newly developed type of optical fiber. One major advantage of POF over glass fiber is that it is inexpensive and simple to install. POF can be used for Gigabit Ethernet and local area networks (LAN) [15], [16]. It can also be used in high definition television (HDTV) and internet protocol television (IPTV) delivery systems [17]. Randel *et al.* [18] provide results with 1 Gbit/s transmission in a step-index POF link using adaptive multiple subcarrier modulation. In our work, we apply optimal rate allocation in the POF channel with OFDM modulation.

The paper is organized as follows. The optimization problem is formulated and solved in Section II. In Section III, the proposed algorithm is applied to image transmission. The two channel models mentioned above are tested. Section IV concludes the paper.

II. Optimization Problem

Suppose that scalable sources are transmitted via fixed-length packets. That is, the total number of bits (info and FEC) is the same for each packet. Suppose further that subchannel m is constrained to transmit exactly N_m channel packets, $m = 1, 2, \ldots, M$. Typically, the N_m are all equal; i.e., $N_m = N_k, \forall m, k$. However, our algorithm is applicable to the more general case where the N_m can be different. The total number of packets to be transmitted is then $N = \sum_{m=1}^{M} N_m$. Define the set of available channel code rates as $\mathcal{R} = \{r_1, r_2, \ldots, r_L\}$ and the set of subchannels as $\mathcal{S} = \{s_1, s_2, \ldots, s_M\}$. A code rate from $\mathcal{R}$ and a subchannel from $\mathcal{S}$ are chosen for each packet. This allocation is denoted by a rate assignment scheme $R = \big((r_{k_1}, s_{g_1}), (r_{k_2}, s_{g_2}), \ldots, (r_{k_N}, s_{g_N})\big)$. Ideally, a rate allocation scheme R is chosen for each packet to minimize the end-to-end expected distortion. However, the distortion-based optimization problem is difficult to solve in the single channel case, and is even more difficult for the multichannel case, since the search space is expanded from L^N to $(LM)^N$. Not only is the search space expanded, but additional constraints arise, such as the constraint on the number of packets for each subchannel as described above. In this paper, we consider an alternative rate-based optimization problem. It has been shown by Hamzaoui *et al.* [19] for the single channel case, that the rate-optimal solution provides a good approximation to the distortion-optimal solution for efficient embedded coders. Chande and Farvardin [20] proposed a rate-optimal solution for fixed-length information blocks (variable length packets). Stankovic *et al.* [12] extended it to fixed-length packets and proposed a fast algorithm. In this paper, we derive a rate-optimal multichannel solution.

The problem can be formulated as follows. Let $E[\cdot]$ denote the expectation operator, and $E_N(R)$ the expected value of the correctly received source length associated with rate assignment scheme R. $L_i(R)$ represents the received source length associated with the event that the first error happens in the $(i+1)^{th}$ packet under rate assignment scheme R, and $P_i(R)$ represents the probability of this event. A rate-optimal error protection scheme (EPS) then maximizes the expected length of correctly received data

$$E_N(R) = \sum_{i=1}^{N} P_i(R) L_i(R) \tag{1}$$

where

$$P_i(R) = p(r_{k_{i+1}}, s_{g_{i+1}}) \sum_{j=1}^{i} (1 - p(r_{k_j}, s_{g_j})) \tag{2}$$

$$L_i(R) = \sum_{j=1}^{i} l(r_{k_j}) \tag{3}$$

and $l(r_{k_j})$ is the number of source bytes in packet j, which is determined by the channel code rate assigned to the packet. Also, $p(r_{k_j}, s_{g_j})$ is the packet error probability of the jth packet when transmitted on channel g_j using code rate k_j. This expression assumes progressive decoding, and that if one or more errors are detected in a channel packet, this packet and all following packets are discarded. Thus, if the first error occurs in the first packet, the amount of correctly received data is zero bytes. Accordingly, $L_0(R) = 0$, so that $i = 0$ need not be included in the sum of (1).

We give two lemmas and two corollaries before we derive the optimal solution. Proofs are given in the Appendix .

Lemma 1: Let $R = \big((r_{k_1}, s_{g_1}), (r_{k_2}, s_{g_2}), \ldots, (r_{k_N}, s_{g_N})\big) \in (\mathcal{R} \times \mathcal{S})^N$ be an N-packet EPS. Then

$$\begin{aligned} &E_N[(r_{k_1}, s_{g_1}), \ldots, (r_{k_N}, s_{g_N})] \\ &\quad = E_1[(r_{k_1}, s_{g_1})] + (1 - p(r_{k_1}, s_{g_1})) \\ &\qquad \times E_{N-1}[(r_{k_2}, s_{g_2}), \ldots, (r_{k_N}, s_{g_N})] \end{aligned} \tag{4}$$

where $E_1[(r_{k_1}, s_{g_1})] = l(r_{k_1})(1 - p(r_{k_1}, s_{g_1}))$.

Lemma 2: If the $(N-1)$-packet EPS $\big((r_2^*, s_2^*), \ldots, (r_N^*, s_N^*)\big)$ is rate optimal, and if

$$\begin{aligned} &E_N[(r_1^*, s_1^*), (r_2^*, s_2^*), \ldots, (r_N^*, s_N^*)] \\ &\qquad \geq E_N[(r_{k_1}, s_{g_1}), (r_2^*, s_2^*), \ldots, (r_N^*, s_N^*)] \end{aligned}$$

for all $r_{k_1} \in \mathcal{R}$, and $s_{g_1} \in \mathcal{S}$, then the N-packet EPS $\left((r_1^*, s_1^*), (r_2^*, s_2^*), \ldots, (r_N^*, s_N^*)\right)$ is rate optimal.

The next two corollaries follow from these lemmas. If the N-packet EPS $\left((r_1^*, s_1^*), \ldots, (r_N^*, s_N^*)\right)$ is rate optimal, then

Corollary 1: For $1 \leq i \leq N-1$, the $(N-i)$-packet EPS $\left((r_{i+1}^*, s_{i+1}^*), \ldots, (r_N^*, s_N^*)\right)$ is rate optimal.

This result shows that an N-packet EPS can be obtained by first calculating 1-packet EPS (which is trivial), and recursively adding one packet $(N-1)$ times.

Corollary 2: Denote subchannel s_n having a smaller bit error rate than s_m by $s_n > s_m$. Then $s_1^* \geq s_2^* \geq \cdots \geq s_N^*$.

From the above two corollaries, the rate-based optimization algorithm can be formulated as follows.

Algorithm:

---

1) Order the M subchannels, s.t. $SC_1 \geq \cdots \geq SC_m \geq \cdots \geq SC_M$. Subchannel SC_m contains N_m packets, and $\sum_{m=1}^{M} N_m = N$.

2) Set $i = 1$, $b = M$, $s_{N-i+1} = SC_b$, and $j_{N-i+1} = \arg\max_{k=1,\ldots,L} E_1[(r_k, SC_M)]$.

3) $i = i + 1$;

If $i = N_b + N_{b+1} + \cdots + N_M + 1$, then $b = b - 1$, $s_{N-i+1} = SC_b$;

If $i = N + 1$, then

$$\{(r_1^*, s_1^*), (r_2^*, s_2^*), \ldots, (r_N^*, s_N^*)\} = \{(r_{j_1}, s_1), (r_{j_2}, s_2), \ldots, (r_{j_N}, s_N)\},$$

and stop.

4)

$$j_{N-i+1} = \arg\max_{k=1,\ldots,L} E_i[(r_k, s_{N-i+1}), (r_{j_{N-i+2}}, s_{N-i+2}), \ldots, (r_{j_N}, s_N)];$$

go to step 3.

Step 1 is initialization, where SC_m denotes the m^{th} ordered subchannel. Step 2 starts the assignment from the worst subchannel SC_M (from Corollary 2), with variable i indexing the packet number. Step 3 and step 4 recursively calculate the N-packet EPS from the 1-packet EPS obtained in step 2 (from Corollary 1). When each of the packets in the current subchannel have been assigned a channel code rate, the packets in the next worst subchannel will be assigned. The procedure continues until all N packets in all M subchannels are assigned code rates.

III. Applications to Image Transmission

In this section, we apply the proposed algorithm to scalable image transmission for two channel models as mentioned previously. Before discussing the two cases individually in Section III-B and C, we describe the image coding and channel coding techniques used in the experiments.

A. Source and Channel Coding

JPEG2000 coded images are used as source images. JPEG2000 [21] is the state-of-the-art image compression standard, which can generate highly scalable codestreams. JEPG2000 divides the subbands from a discrete wavelet transform into rectangular regions called codeblocks. Each bitplane of each codeblock is coded into a number of (compressed) coding passes. Generally, an image is encoded into multiple layers. Each layer contains differing numbers of coding passes from each codeblock. During the encoding procedure, a distortion-rate slope is computed for each coding pass. The distortion-rate slope values characterize the contribution of the coding pass to the quality of the image. Coding passes with larger slope values are more important than those with smaller slope values. A slope threshold is generated to guide the assembly of one layer. All coding passes having slope values larger than the threshold are included in that layer. Hence, these thresholds identify the importance of layers. Consecutive layers have slope thresholds (importance) in descending order. The coding passes in each layer are collected into a number of JPEG2000 packets. These packets are not to be confused with the channel packets described in previous sections. At the beginning of a codestream, there is a main header, which contains crucial information for the decoder to decode the codestream correctly. Similarly, each JPEG2000 packet has a packet header. The optional JPEG2000 packed packet header marker segments (PPM) are used in our experiments to move all JEPG2000 packet headers to the main header. The main header (including the relocated packet headers) is then assigned the lowest code rate (highest protection).

In what follows, we consider the case where multiple images are transmitted through a common channel. These images may be entirely unrelated. However, in Part III of the JPEG2000 standard (referred to as Motion JPEG2000), each frame of a video sequence is compressed independently. Thus, the multiple images transmitted through the channel (using our proposed system) could be frames of a video sequence. We examine two methods to transmit multiple images. We first consider transmitting each image with an equal number of channel packets. For example, if 256 packets are used to transmit four images, each image occupies 64 packets. In this case, the total available resources are divided equally. We next consider multiplexing the images together and adjusting the available resources among the images according to their characteristics. The multiplexing is done by combining all the layers from all the images. Accordingly, the source encoder first encodes all the images individually. The slope values of all layers from each image are recorded for future ordering purposes. The ownership of each layer and the length of the layer are sent as side information. A "pseudo" image is assembled by concatenating the main headers of all the images together, followed by the layers ordered by slope thresholds. Packetization and rate allocation can then be performed on the "pseudo" image using the algorithm described in Section II.

At the channel output, the "pseudo" image is split into individual images, each of which is decoded separately by a JPEG2000 decoder. If incorrect decoding is detected (by CRC) in a channel packet, this packet and all the following packets

TABLE I
AVERAGE MSE AND PSNR FOR PARALLEL GAUSSIAN CHANNELS

0.5 bpp/source										
	Scheme I		Scheme II		Scheme III		Scheme IV		Scheme V	
	MSE	PSNR	MSE	PSNR	MSE	PSNR	MSE	PSNR	MSE	PSNR
Lena	68.66	29.76	86.74	28.75	26.41	33.91	30.06	33.35	90.61	28.56
Goldhill	102.01	28.04	133.53	26.88	54.59	30.76	63.26	30.12	135.73	26.80
Whitehouse	289.71	23.51	354.77	22.63	355.67	22.62	419.24	21.91	367.72	22.48
Lighthouse	470.34	21.41	545.16	20.77	655.16	19.97	716.13	19.58	616.18	20.24
Average	232.68	24.46	280.05	23.66	272.96	23.77	307.17	23.26	302.56	23.33
1.0 bpp/source										
	Scheme I		Scheme II		Scheme III		Scheme IV		Scheme V	
	MSE	PSNR	MSE	PSNR	MSE	PSNR	MSE	PSNR	MSE	PSNR
Lena	48.64	31.26	55.86	30.66	11.87	37.39	13.72	36.76	56.28	30.63
Goldhill	74.89	29.39	89.32	28.62	28.87	33.53	34.30	32.78	91.68	28.51
Whitehouse	186.37	25.43	214.55	24.82	206.95	24.97	238.44	24.36	226.34	24.58
Lighthouse	177.61	25.64	253.50	24.09	440.83	21.69	489.96	21.23	309.07	23.23
Average	121.88	27.27	153.31	26.28	172.13	25.77	194.11	25.25	170.84	25.80

are discarded. This policy is based on the assumption that later packets cannot be used without the reception of earlier packets. This assumption is not strictly satisfied since an error in one image will not affect the decoding of another image. Thus, decoding can be continued for any image that does not contribute bytes to the incorrectly decoded packet. Nevertheless, we adopt the stated policy in our experiments. The reason for this is primarily simplicity. Also, in our experiments, we use four images, each encoded with 50 layers. As a result, at least two (frequently three) images contribute to each channel packet. Therefore, gains achievable by the more complicated policy are expected to be small.

Rate-compatible punctured turbo codes (RCPT) are employed as channel codes. A rate 1/3 parallel concatenated convolutional code with generator polynomial (33,31) is chosen as the encoder. A puncturing period of eight is used. A maximum number of 20 iterations are used for decoding. Channel packets of length 512 bytes are used. Four bytes are reserved for a 32-bit CRC, which is used for error detection following turbo decoding. One byte is reserved for transmitting side information such as the turbo code rate. Code rates are chosen from the set $\mathcal{R} = \{8/9, 8/10, \ldots, 8/23, 8/24\}$. The cardinality of this set is 16. The following subsections discuss transmission for the two different channel models.

B. Independent Parallel Gaussian Channels

As a first example, independent parallel Gaussian channels are assumed. BPSK modulation is used. Four greylevel 512×512 images are used as source images: Lena, Goldhill, Whitehouse, and Lighthouse. We choose 32 AWGN channels with equally spaced SNRs between 1.0 and 3.0 dB.

There are five error protection schemes tested in the experiments. The first is a UEP scheme. Multiple source images are multiplexed together using the method described in Section III-A. Then the rate allocation algorithm described in Section II is used to assign a channel and code rate to each packet. This scheme is denoted as Scheme I henceforth. The second scheme is an EEP scheme, denoted by Scheme II. In Scheme II, multiple source images are multiplexed as in Scheme I. However, data from the "pseudo" image is packed into packets, each of which is protected by the same code, with a code rate equal to the average code rate used in Scheme I. This scheme is denoted as Scheme II. Next, we consider a UEP scheme, in which images are not multiplexed together. This scheme is denoted as Scheme III. In this scheme, the images are not multiplexed. Rather, each source image is assigned the same number of channel packets from each subchannel. Before transmission of each image, the rate allocation algorithm introduced in Section II is first used to assign subchannels and code rates to all the packets of that image. In Scheme IV, images are not multiplexed, and all packets are protected by the same code, with a code rate equal to the average code rate used in Scheme III. Schemes III and IV can be thought of as time division schemes. That is, the first image can be thought of as being transmitted using all channels, followed by the second image, and so on. Scheme III optimizes the use of the channels (UEP) while Scheme IV does not (EEP). Last, Scheme V is tested. In this scheme, images are multiplexed as in Scheme I. However, instead of using the true SNRs of all the subchannels, an average channel SNR is used in the rate allocation algorithm. In this scheme, a 2.0-dB channel is assumed for allocating all N packets. In all the schemes, headers are protected by a code of rate 1/3.

Simulation results are listed in Table I. A total number of $N = 128$ packets are used for an average rate of 0.5 bpp/source, including all header and parity info. Similarly, $N = 256$ packets are used for an average rate of 1.0 bpp/source. Each case is simulated 1000 times. The resulting MSE values for each case are averaged and then converted to PSNR values. Similarly, the row labelled "Average" is MSE averaged over all simulations and all images and then converted to PSNR. This method has been adopted in several recent studies [7], [22], [23] and has been shown to correlate well with visual quality [24]. UEP gains can be observed by comparing results from Scheme I with Scheme II (about 0.8 to 1 dB), and Scheme III with Scheme IV (about 0.5 dB). Source multiplexing gains can be observed by comparing results from Scheme I with Scheme III, and Scheme II with Scheme IV. These gains come from differing numbers of packets being allocated between different sources according to their characteristics. The total gain from both multiplexing and UEP is about 1.2 dB at 0.5 bpp/source, and 2.0 dB at 1.0 bpp/source. It can also be observed that the proposed multiplexing tends to give a more fair QoS among

TABLE II
AVERAGE MSE AND PSNR FOR 1.0 BPP/SOURCE AND GI-POF CHANNEL

	Scheme I		Scheme II		Scheme III		Scheme IV	
	MSE	PSNR	MSE	PSNR	MSE	PSNR	MSE	PSNR
Lena	41.16	31.99	55.07	30.72	12.04	37.33	12.79	37.06
Goldhill	67.81	29.82	89.83	28.60	27.15	33.79	31.73	33.12
Whitehouse	158.07	26.14	208.69	24.94	193.74	25.26	232.37	24.47
Lighthouse	172.15	25.77	205.70	25.00	419.93	21.90	477.37	21.34
Average	109.80	27.72	139.82	26.68	163.21	26.00	188.56	25.38

multiple sources in the sense that the MSE differences are significantly reduced. Comparing Schemes I and V, it can be observed that significant gains (about 1.1 dB for 0.5 bpp/source and 1.5 dB for 1.0 bpp/source) are achieved by fully utilizing the individual characteristics of all subchannels, rather than simply designing for the "average" channel.

C. Plastic Optical Fiber Channel

Next, a graded-index plastic optical fiber (GI-POF) channel model with OFDM modulation is considered as the second example. The impulse response of GI-POF can be modelled as [25] $h(t) = (1/\sqrt{2\pi\alpha^2})\exp(-t^2/2\alpha^2)$. Its transfer function is $H(\omega) = \exp(-\alpha^2\omega^2/2)$, where $\alpha = \sqrt{2\ln 2}T_b/2\pi f_n$, T_b is the pulse coded modulation (PCM) bit time, and f_n is the channel bandwidth normalized to the PCM data rate.

OFDM modulation is considered. A brief introduction of OFDM is presented here. The information sequence is subdivided into K groups (subchannels). For coded OFDM systems, information bits are first passed through a channel encoder for each subchannel. The OFDM modulator consists of K independent subchannels. K signal points, X_k, are chosen from certain constellations according to any phase shift keying (PSK) or quadrature amplitude modulation (QAM) signaling set (symbol mapping). BPSK modulation is used in our experiments. Those symbols can be viewed as values of the discrete Fourier transform (DFT) of an OFDM signal $x(t)$. A cyclic prefix is appended to avoid intersymbol interference (ISI). The signal is transmitted through some channel after D/A conversion. The received signal may be expressed as $r(t) = x(t) \star h(t) + n(t)$, where $\star$ represents convolution, and $n(t)$ is additive noise corrupting the signal. At the receiver end, inverse procedures are taken to recover estimates of the original information bits.

In our experiments, we employ the GI-POF channel. The nonflat shape of the transfer function of the POF channel causes the subchannels to have different channel gains. In particular, the signal $x(t)$ is convolved with the impulse response of the channel. Equivalently, the subchannel symbols X_k are multiplied by the transfer function of the channel. We assume AWGN with SNR denoted by γ_0. The gain ρ_k of each subchannel can be computed from the transfer function. The SNR of each subchannel is then computed as $\gamma_k = \rho_k^2\gamma_0$. The same image sources are used as in the previous example. In the experiments, the OFDM system has 128 subchannels. A channel SNR of $\gamma_0 = 3$ dB and $f_n = 1.3$ are selected. The bit rate of the system is 2.5 Gb/s, and a total of 256 packets are transmitted. The results are listed in Table II. Similar conclusions can be drawn to those of the previous example. The total gain from multiplexing and UEP is about 2.3 dB.

IV. CONCLUSION

In this paper, a multichannel rate allocation algorithm is proposed. A fast algorithm assigns unequal error protection to each segment of a source to maximize the expected value of the correctly received source length. Differences between subchannels are fully utilized. The algorithm can be applied to many systems that suffer from nonideal channels. Applications to JPEG2000 transmission shows the benefits of the proposed algorithm obtained by exploiting the differences between subchannels instead of using the average subchannel SNR. Significant UEP gains are achieved over EEP schemes. The rate allocation algorithm is independent of the transmitted source, but additional performance gains can be obtained by multiplexing multiple sources prior to rate allocation.

APPENDIX

Proof of Lemma 1:

$$\begin{aligned}
&E_N[(r_{k_1}, s_{g_1}), \ldots, (r_{k_N}, s_{g_N})] \\
&= l(r_{k_1})\sum_{i=1}^{N} P_i(R) + \sum_{i=2}^{N} P_i(R)\sum_{j=2}^{i} l(r_{k_j}) \\
&= l(r_{k_1})(1 - p(r_{k_1}, s_{g_1})) + \sum_{i=2}^{N} P_i(R)\sum_{j=2}^{i} l(r_{k_j}) \\
&= l(r_{k_1})(1 - p(r_{k_1}, s_{g_1})) + (1 - p(r_{k_1}, s_{g_1})) \\
&\quad E_{N-1}[(r_{k_2}, s_{g_2}), \ldots, (r_{k_N}, s_{g_N})].
\end{aligned}$$

Proof of Lemma 2:

$$\begin{aligned}
&E_N[(r_1^*, s_1^*), (r_2^*, s_2^*), \ldots, (r_N^*, s_N^*)] \\
&\geq (1 - p(r_{k_1}, s_{g_1}))[l(r_{k_1}) + E_{N-1}[(r_2^*, s_2^*), \ldots, (r_N^*, s_N^*)] \\
&\geq (1 - p(r_{k_1}, s_{g_1}))[l(r_{k_1}) + E_{N-1}[(r_{k_2}, s_{g_2}), \ldots, (r_{k_N}, s_{g_N})] \\
&= E_N[(r_{k_1}, s_{g_1}), (r_{k_2}, s_{g_2}), \ldots, (r_{k_N}, s_{g_N})].
\end{aligned}$$

Proof of Corollary 1:

$$\begin{aligned}
&E_N[(r_1^*, s_1^*), (r_2^*, s_2^*), \ldots, (r_N^*, s_N^*)] \\
&\qquad \geq E_N[(r_1^*, s_1^*), (r_{k_2}, s_{g_2}), \ldots, (r_{k_N}, s_{g_N})]
\end{aligned}$$

which implies

$$\begin{aligned}
&E_1[(r_1^*, s_1^*)] + (1 - p(r_1^*, s_1^*))E_{N-1}[(r_2^*, s_2^*), \ldots, (r_N^*, s_N^*)] \\
&\geq E_1[(r_1^*, s_1^*)] + (1 - p(r_1^*, s_1^*))E_{N-1}[(r_{k_2}, s_{g_2}), \ldots, (r_{k_N}, s_{g_N})].
\end{aligned}$$

This in turn yields

$$\begin{aligned}
&E_{N-1}[(r_2^*, s_2^*), \ldots, (r_N^*, s_N^*)] \\
&\qquad \geq E_{N-1}[(r_{k_2}, s_{g_2}), \ldots, (r_{k_N}, s_{g_N})].
\end{aligned}$$

Similarly, we can get

$$E_{N-i}[(r^*_{i+1}, s^*_{i+1}), \ldots, (r^*_N, s^*_N)] \geq E_{N-i}[(r_{k_{i+1}}, s_{g_{i+1}}), \ldots, (r_{k_N}, s_{g_N})].$$

Proof of Corollary 2: From *Corollary 1*, we have $E_2[(r^*_{N-1}, s^*_{N-1}), (r^*_N, s^*_N)] \geq E_2[(r^*_{N-1}, s^*_N), (r^*_N, s^*_N)]$. By (4), we obtain

$$E_1[(r^*_{N-1}, s^*_{N-1})] + (1 - p(r^*_{N-1}, s^*_{N-1}))E_1[(r^*_N, s^*_N)] \geq E_1[(r^*_{N-1}, s^*_N)] + (1 - p(r^*_{N-1}, s^*_N))E_1[(r^*_N, s^*_N)]$$

which indicates that

$$E_1[(r^*_{N-1}, s^*_N)] - E_1[(r^*_{N-1}, s^*_{N-1})] \leq (p(r^*_{N-1}, s^*_N) - p(r^*_{N-1}, s^*_{N-1}))E_1[(r^*_N, s^*_N)]. \quad (5)$$

If $s^*_N > s^*_{N-1}$, then (5) has $RHS < 0$ and $LHS > 0$, which is a contradiction. Thus, we must have $s^*_{N-1} \geq s^*_N$. Similarly

$$E_3[(r^*_{N-2}, s^*_{N-2}), (r^*_{N-1}, s^*_{N-1}), (r^*_N, s^*_N)] \geq E_3[(r^*_{N-2}, s^*_{N-1}), (r^*_{N-1}, s^*_{N-1}), (r^*_N, s^*_N)]$$

which yields

$$\{E_1[(r^*_{N-2}, s^*_{N-2})] + (1 - p(r^*_{N-2}, s^*_{N-2}))E_2[(r^*_{N-1}, s^*_{N-1}) (r^*_N, s^*_N)] \geq E_1[(r^*_{N-2}, s^*_{N-1})] + (1 - p(r^*_{N-2}, s^*_{N-1})) E_2[(r^*_{N-1}, s^*_{N-1}), (r^*_N, s^*_N)].$$

This leads to

$$E_1[(r^*_{N-2}, s^*_{N-1})] - E_1[(r^*_{N-2}, s^*_{N-2})] \leq (p(r^*_{N-2}, s^*_{N-1}) - p(r^*_{N-2}, s^*_{N-2})) E_2[(r^*_{N-1}, s^*_{N-1}), (r^*_N, s^*_N)]. \quad (6)$$

By the same argument as above, we obtain $s^*_{N-2} \geq s^*_{N-1}$. The same method can be used to show that $s^*_{i-1} \geq s^*_i$, for $2 \leq i \leq N$.

References

[1] J. A. C. Bingham, "Multicarrier modulation for data transmission: An idea whose time has come," *IEEE Commun. Mag.*, vol. 28, no. 5, pp. 5–14, May 1990.

[2] I. Kalet, "The multitone channel," *IEEE Trans. Commun.*, vol. 37, no. 2, pp. 119–124, Feb. 1989.

[3] S. S. Pradhan and K. Ramchandran, "Optimized embedded multicarrier modulation for efficient delivery of layered video data," in *Proc. IEEE Int. Conf. Communications*, Jun. 1998, vol. 2, pp. 1009–1012.

[4] P. J. Cherriman, T. Keller, and L. Hanzo, "Subband-adaptive turbo-coded OFDM-based interactive video telephony," *IEEE Trans. Circuits, Syst., Video Technol.*, vol. 12, no. 10, pp. 829–839, Oct. 2002.

[5] J. Song and K. J. R. Liu, "Robust progressive image transmission over OFDM systems using space-time block code," *IEEE Trans. Multimedia*, vol. 4, no. 3, pp. 394–406, Sep. 2002.

[6] Y. Sun, Z. Xiong, and X. Wang, "Scalable image transmission over differentially space-time coded OFDM systems," in *Proc. Global Telecommunications Conf.*, Nov. 2002, pp. 379–383.

[7] Y. Sun and Z. Xiong, "Progressive image transmission over space-time coded OFDM-based MIMO systems with adaptive modulation," *IEEE Trans. Mobile Comput.*, vol. 4, no. 8, pp. 1016–1028, Aug. 2006.

[8] Y. S. Chan, P. C. Cosman, and L. B. Milstein, "A cross-layer diversity technique for multicarrier OFDM multimedia networks," *IEEE Trans. Image Process.*, vol. 15, no. 4, pp. 833–847, Apr. 2006.

[9] H. Zheng and K. J. R. Liu, "Robust image and video transmission over spectrally shaped channels using multicarrier modulation," *IEEE Trans. Multimedia*, vol. 1, pp. 88–103, Mar. 1999.

[10] S. Zhao, Z. Xiong, and X. Wang, "Optimal resource allocation for wireless video over CDMA networks," *IEEE Trans. Mobile Comput.*, vol. 4, no. 1, pp. 56–67, Jan./Feb. 2006.

[11] S. Zhao, Z. Xiong, X. Wang, and J. Hua, "Progressive video delivery over wideband wireless channels using space-time differentially coded OFDM systems," *IEEE Trans. Mobile Comput.*, vol. 5, no. 4, pp. 303–316, Apr. 2006.

[12] V. Stankovic, R. Hamzaoui, and D. Saupe, "Fast algorithm for rate-based optimal error protection of embedded codes," *IEEE Trans. Commun.*, vol. 51, no. 11, pp. 1788–1795, Nov. 2003.

[13] Radio Broadcast Systems, Digital Audio Broadcasting (DAB) to Mobile, Portable and Fixed Receivers, ETS 300 401, 1994.

[14] Digital Broadcasting Systems for Television, Sound and Data Services, Framing Structure, Channel Coding and Modulation for Digital Terrestrial Television, ETS 300 744, 1997.

[15] F. Mederer, R. Jäger, P. Schnitzer, H. Unold, M. Kicherer, K. J. Ebeling, M. Naritomi, and R. Yoshida, "Multi-Gb/s graded-index POF data link with butt-coupled single-mode InGaAs VCSEL," *IEEE Photon. Technol. Lett.*, vol. 12, no. 2, pp. 199–201, Feb. 2000.

[16] T. Matsuoka, T. Ito, and T. Kaino, "First plastic optical fibre transmission experiment using 520 nm LEDs with intensity modulation/direct detection," *IEE Electron. Lett.*, vol. 36, pp. 1836–1837, Oct. 2000.

[17] [Online]. Available: http://www.technologynewsdaily.com/node/2927

[18] S. Randel, S. C. J. Lee, B. Spinnler, F. Breyer, H. Rohde, J. Walewski, A. M. J. Koonen, and A. Kirstädter, "1 Gbit/s transmission with 6.3 bit/s/hz spectral efficiency in a 100 m standard 1 mm step-index plastic optical fibre link using adaptive multiple sub-carrier modulation," in *Proc. 32nd Eur. Conf. Optical Communication*, Sep. 2006, pp. 41–42.

[19] R. Hamzaoui, V. Stankovic, and Z. Xiong, "Rate-based versus distortion-based optimal joint source-channel coding," in *Proc. Data Compression Conf.*, Snowbird, UT, Apr. 2002, pp. 63–72.

[20] V. Chande and N. Farvardin, "Progressive transmission of images over memoryless noisy channels," *IEEE J. Sel. Areas Commun.*, vol. 18, no. 6, pp. 850–860, Jun. 2000.

[21] D. S. Taubman and M. W. Marcellin, *JPEG2000: Image Compression Fundamentals, Standards and Practice*. Norwell, MA: Kluwer, 2002.

[22] T. Chuu, Z. Liu, Z. Xiong, and X. Wu, "Joint UEP and layered source coding with application to transmission of JPEG2000 coded images," in *Proc. Global Comm. Conf.*, 2001, vol. 3, pp. 2036–2039.

[23] Z. Wu, A. Bilgin, and W. M. Marcellin, "Joint source/channel coding for image transmission with JPEG2000 over memoryless channels," *IEEE Trans. Image Process.*, vol. 14, no. 8, pp. 1020–1032, Aug. 2005.

[24] M. Kalman and B. Girod, "Optimal channel-time allocation for the transmission of multiple video streams over a shared channel," in *Proc. IEEE 7th Workshop on Multimedia Signal Processing*, Oct. 2005, pp. 1–4.

[25] B.-G. Shin, J.-H. Park, and J.-J. Kim, "Low-loss, high-bandwidth graded-index plastic optical fiber fabricated by the centrifugal deposition method," *Appl. Phys. Lett.*, vol. 82, no. 26, pp. 4645–4647, Jun. 2003.

Lingling Pu (S'05) received the B.S. degree in electrical engineering and information science from University of Science and Technology of China in 1999 and the M.S. degree in electrical engineering from North Dakota State University, Fargo, in 2002. She is currently pursuing the Ph.D. degree in electrical engineering at the University of Arizona, Tucson.

Her research interests include image processing, joint source/channel coding, and digital signal processing.

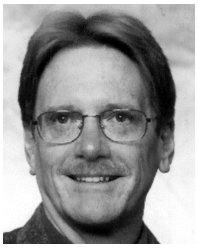

Michael W. Marcellin (S'81–M'87–SM'93–F'02) was born in Bishop, CA, in 1959. He received the B.S. degree in electrical engineering (summa cum laude) from San Diego State University, San Diego, CA, in 1983, where he was named the most outstanding student in the College of Engineering, and the M.S. and Ph.D. degrees in electrical engineering from Texas A&M University, College Station, in 1985 and 1987, respectively.

Since 1988, he has been with the University of Arizona, where he is a Regents Professor of electrical and computer engineering and optical sciences. He is a major contributor of technology to JPEG2000, the emerging second-generation standard for image compression. Throughout the standardization process, he chaired the JPEG2000 Verification Model Ad Hoc Group, in which was responsible for the software implementation and documentation of the JPEG2000 algorithm. He is coauthor of the book (with D. S. Taubman) *JPEG2000: Image Compression Fundamentals, Standards and Practice* (Kluwer, 2002). This book is intended to serve as a textbook on image compression fundamentals, as well as the definitive reference on JPEG2000. He served as a Consultant to Digital Cinema Initiatives (DCI), a consortium of Hollywood studios, on the development of the JPEG2000 profiles for digital cinema applications. His research interests include digital communication and data storage systems, data compression, and signal processing. He has authored or coauthored more than 180 publications in these areas.

Prof. Marcellin is a member of Tau Beta Pi, Eta Kappa Nu, and Phi Kappa Phi. He is a 1992 recipient of the National Science Foundation Young Investigator Award, and a corecipient of the 1993 IEEE Signal Processing Society Senior (Best Paper) Award. He has received teaching awards from NTU (1990, 2001), IEEE/Eta Kappa Nu student sections (1997), and the University of Arizona College of Engineering (2000). He is also the recipient of the 2006 University of Arizona Technology Innovation Award. From 2001 to 2006, he was the Litton Industries John M. Leonis Distinguished Professor of Engineering at the University of Arizona. He is currently the International Foundation for Telemetering Distinguished Professor of Electrical and Computer Engineering.

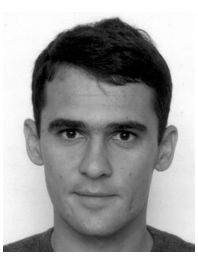

Ivan Djordjevic (M'04) is an Assistant Professor of Electrical and Computer Engineering at the University of Arizona, Tucson. Prior to this appointment in August 2006, he was with University of Arizona, Tucson, University of the West of England, Bristol, U.K.; University of Bristol, Bristol, U.K.; Tyco Telecommunications, Eatontown, NJ; and the National Technical University of Athens, Athens, Greece. His current research interests include fiber-optic communication systems and networks, error control coding, constrained coding, coded modulation, turbo equalization and OFDM. He is author of more than 100 international publications.

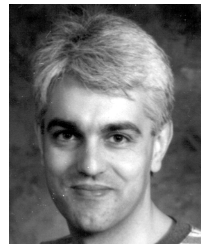

Bane Vasic (S'92–M'93–SM'02) is an Associate Professor of electrical and computer engineering and mathematics at the University of Arizona, Tucson. Prior to this appointment, he was at Bell Laboratories. He developed a decoding algorithm that is implemented in virtually all of today's magnetic hard drives. His research interests include coding theory, communication theory, and constrained systems.

Prof. Vasic is a Co-Chair of the IEEE Communication Workshop (CTW 2007). He was a Co-Chair of the Communication Theory Symposium of the IEEE International Conference on Communications (ICC 2006). He recently organized the Workshop on Theoretical Advances in Information Recording and the Los Alamos Workshop on Applications of Statistical Physics to Coding Theory.

Ali Bilgin (S'94–M'03) received the B.S. degree in electronics and telecommunications engineering from Istanbul Technical University, Istanbul, Turkey, the M.S. degree in electrical engineering from San Diego State University, San Diego, CA, and the Ph.D. degree in electrical engineering from the University of Arizona, Tucson.

He is currently a Research Assistant Professor with the Department of Electrical and Computer Engineering at the University of Arizona. His current research interests are in the areas of signal and image processing and include image and video coding, data compression, and magnetic resonance imaging. He has coauthored over 85 research papers in these areas.